ACS APPLIED MATERIALS & INTERFACES

Research Article

www.acsami.org

Facile Fabrication of Scalable, Hierarchically Structured Polymer/Carbon Architectures for Bioelectrodes

Heather R. Luckarift,*[,†,‡] Susan R. Sizemore,[†,‡] Karen E. Farrington,[†,‡] Jared Roy,[§] Carolin Lau,[§] Plamen B. Atanassov,[§] and Glenn R. Johnson*[,†]

[†]Microbiology and Applied Biochemistry Laboratory, Air Force Research Laboratory, Materials and Manufacturing Directorate (AFRL/RXQL), Tyndall Air Force Base, Florida 32403, United States

[‡]Universal Technology Corporation, 1270 North Fairfield Road, Dayton, Ohio 45434, United States

[§]Center for Emerging Energy Technologies and Department of Chemical and Nuclear Engineering, University of New Mexico, Albuquerque, New Mexico 87131, United States

ABSTRACT: This research introduces a method for fabrication of conductive electrode materials with hierarchical structure from porous polymer/carbon composite materials. We describe the fabrication of (3-hydroxybutyrate-*co*-3-hydroxyvalerate) (PHBV) scaffolds doped with carbon materials that provide a conductive three-dimensional architecture that was demonstrated for application in microbial fuel cell (MFC) anodes. Composite electrodes from PHBV were fabricated to defined dimensions by solvent casting and particulate leaching of a size-specific porogen (in this case, sucrose). The cellular biocompatibility of the resulting composite material facilitated effective immobilization of a defined preparation of *Shewanella oneidensis* DSP-10 as a model microbial catalyst. Bacterial cells were immobilized via chemical vapor deposition (CVD) of silica to create an engineered biofilm that exhibits efficient bioelectrocatalysis of a simple-carbon fuel in a MFC. The functionalized PHBV electrodes demonstrate stable and reproducible anodic open circuit potentials of −320 ± 20 mV (vs Ag/AgCl) with lactate as the electron donor. Maximum power densities achieved by the hierarchically structured electrodes (~5 mW cm^3) were significantly higher than previously observed for graphite-felt electrodes. The methodology for fabrication of scalable electrode materials may be amenable to other bioelectrochemical applications, such as enzyme fuel cells and biosensors, and could easily be adapted to various design concepts.

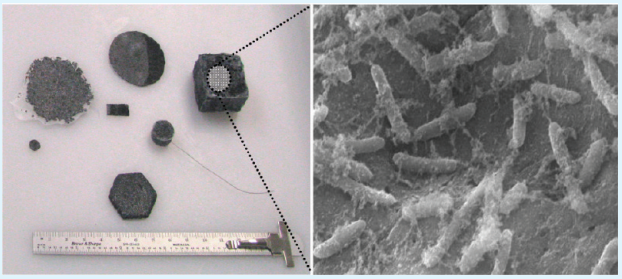

KEYWORDS: *hierarchically structured electrodes, porous polymer/carbon composites, microbial fuel cells, biological fuel cells, Shewanella oneidensis DSP-10, bioelectrochemistry*

INTRODUCTION

Recent advances in bioelectrochemical systems are products of deeper understanding of biological redox processes along with new materials and methodologies to control the bionano interface.[1] Microbial fuel cells (MFC) are an outstanding experimental and developmental model of bioelectrochemical systems; the MFC integrate controlled bioprocesses with energy harvesting and power generation technology to provide a complex system with practical aspects. In a typical MFC anode, dissimilatory metal-reducing bacteria convert chemical energy to electrical energy by transferring electrons from reduced electron donors (e.g., lactate) to insoluble electron acceptors (i.e., the electrode surface).[2] In nature, bacteria maximize the use of insoluble electron acceptors (usually Fe or Mn oxides) by excreting extracellular polymers that serve to bind the growing cell population into a structured biofilm.[3,4] Biofilms, however, require significant time to become established, which often leads to variable and irreproducible power density when applied to MFC design.[5] The variability of natural biofilm formation can be circumvented, however, by attaching bacteria in a manner that preserves the integrity of whole cells and defines the number, activity and physiological status of the initial bacterial population.[6] Encapsulating a defined population of cells in a silica matrix mimics the natural phenomenon, and provides a rapid and controlled approach to defining an "artificial biofilm".[6] Such engineered biofilms can benefit from designing MFC or devices that integrate bacterial cultures in general, and provide a unique opportunity to fabricate devices with microbial communities that are not traditional biofilm formers. Moreover, the approach may be applied to effectively "seed" a surface with any desired microbial community.[7]

Achieving efficient energy transfer from the microbial cells of an MFC biofilm requires an electrode material that is conductive, yet biocompatible, in order to provide an interface for bacterial interactions. Numerous conductive and carbona-

Received: January 9, 2012
Accepted: March 7, 2012
Published: March 7, 2012

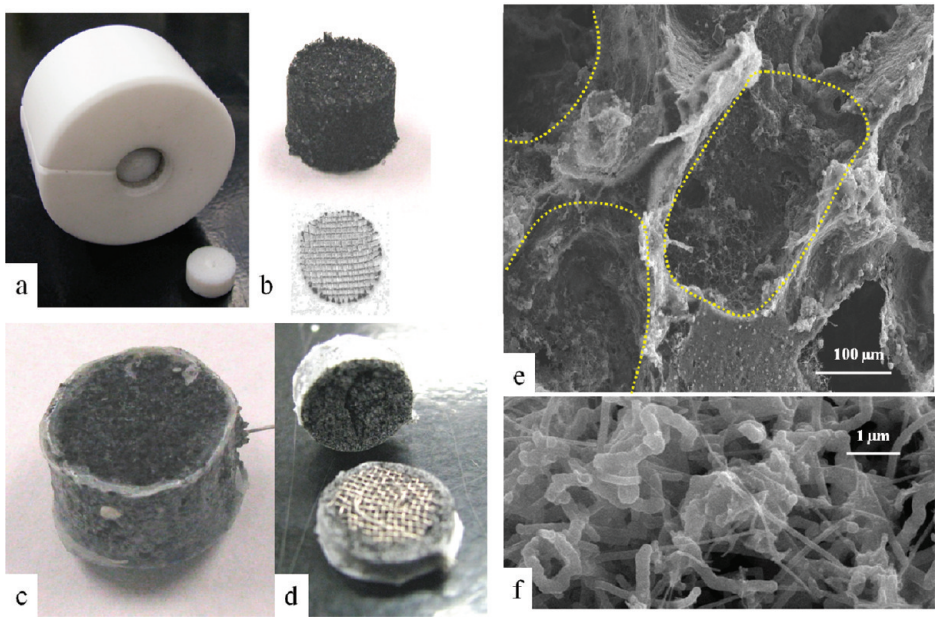

Figure 1. Schematic of polymer/carbon (PHBV/CF) composite fabrication. (a) A die is used to (b) pack sucrose/CF around a nickel mesh. (c) The resulting sucrose/CF scaffold is intercalated with polymer and (d) the sucrose removed to form a porous scaffold. Final electrode cut to show the interior nickel mesh. (e) The sucrose dissolves and leaves a hole of a size comparable to the original particles (yellow dashed lines) that is (f) interconnected with carbon fibers.

ceous materials have been investigated to support anodic reactions in MFC development.[2,8] Many potential anode materials, however, are restricted in application by limitations in scalability, cost-effectiveness, conforming dimensions, and manufacturability.[9] Fabricating conductive scaffolds from biopolymers may provide a technology approach to make three-dimensional composites with tailored structural and mechanical properties. It is desired for such materials to have hierarchical architectures with structured porosity in order to provide ready nutrient access through a large pore volume. At the same time, the architecture requires sufficient surface area to allow a high cell density to be immobilized in a minimal volume in order to maximize the volumetric power density of the MFC. Attempts to form conductive matrices with integrated biopolymers such as chitosan and cellulose when doped with carbon nanotubes have charted the onset of such a materials design strategy.[10−13]

Bacteria excrete a wide variety of biopolymers that are used in the development of a new class of materials called bioplastics.[14] Polyhydroxyalkanoates (PHA), such as poly (3-hydroxybutyrate) (PHB) and (3-hydroxybutyrate-*co*-3-hydroxyvalerate) (PHBV), are extracellular monomers that serve as carbon and energy stores for bacterial cells.[14,15] These biological polymers are biocompatible with a wide variety of cell types and therefore find application in tissue engineering.[16] Adding extra functionality to bioplastics extends the versatility of the polymer scaffolds to applications such as drug delivery and biosensing. PHA composites that include ceramic particles for enhanced mechanical strength, antioxidative vitamins to enhance biocompatibility, or composites with added carbonaceous materials to provide conductive properties, have all been demonstrated.[17−24]

PHA polymers are stable under typical MFC conditions (neutral pH and ambient temperatures), inexpensive and can be fabricated to conform with shapes and scale of various applications. In addition, the biocompatible properties of the polymer encourage cellular retention and provide a scaffold that is amenable to flow through configurations. The porosity of PHA can be controlled by careful choice of the scaffold template. In most cases, a water-soluble, low-molecular-weight species provides the template or "porogen". Simple solvent casting and particulate leaching of sucrose, for example, provides rapid templating of a predetermined architecture.[18] The characteristics of scaffold architecture of a conductive PHA composite are experimentally defined below in respect to anode performance with *Shewanella oneidensis* DSP-10 as a model organism and used to demonstrate a facile method for fabricating highly reproducible, easily integrated and stable MFC anodes.[25]

MATERIALS AND METHODS

Chemicals. Poly (3-hydroxybutyrate-*co*-3-hydroxyvalerate) (PHBV) with 12% poly (hydroxyvalerate) content, and graphitized carbon nanofibers (CF; hollow fibers 80−200 mm o.d., 0.5−10 nm i.d., length 0.5−20 μm) were purchased from Sigma-Aldrich (St. Louis, MO). Sucrose was purchased as a general grocery item as common household sugar and sieved to a defined size using 30−60 mesh screen sieves (0.250−0.595 mm particle size).

Preparation of PHBV/CF Scaffolds. Wet sucrose was mixed with CF (100:1 w/w), hand-pressed into cylindrical prefabricated molds (1.3 × 0.9 cm; volume = 1.195 cm^3) and dried overnight at 37 ^oC. All sucrose/CF mixtures were pressed around a circle of nickel screen (40 mesh, Alfa Aeser, Ward Hill, MA) to act as a current collector that was connected externally via a length of titanium wire (0.25 mm diameter, Goodfellow, Oakdale, PA). PHBV was dissolved in chloroform (0.04% w/v), heated to 60 °C and applied to the sucrose/CF template until all of the PHBV solution was incorporated. After overnight drying at 25 ^oC, the resulting polymer composite (PHBV/CF) was immersed in deionized water (0.3 L) for 2 h to dissolve the sucrose (Figure 1). The resulting composite electrodes are designated as $PHBV_{30}$/CF and $PHBV_{45}$/CF for PHBV/CF composites formed with 30 and 45 mesh size sucrose respectively.

Growth and Immobilization of *Shewanella oneidensis* DSP-10. *S. oneidensis* DSP-10 was cultured in Luria−Bertani broth containing rifampicin (5 $\mu g\ mL^{-1}$) at 30 ^oC, 150 rpm. Cell counts

were determined by conventional serial dilution, plating and counts of colony forming units per mL (cfu mL^{-1}). Cells were harvested at late stationary phase (OD_{600} ~4−5), washed (x 3) and resuspended in phosphate buffered saline (8 g L^{-1} NaCl, 0.2 g L^{-1} KCl, 1.44 g L^{-1} Na_2HPO_4, 0.24 g L^{-1} KH_2PO_4, pH 7.4) to a defined cell density (1×10^9 cfu mL^{-1}). DSP-10 was immobilized to the PHBV/CF composite electrodes using a method for silica-encapsulation described previously (6). Briefly, PHBV/CF electrodes were placed in a glass Petri dish (4.5 cm diameter) modified with a central glass well (1.7 cm diameter) to accommodate the electrode. The cell suspension (1 mL) was added to cover the PHBV/CF electrode and tetramethylorthosilicate (TMOS; 0.2 mL) was added to the outer well. TMOS in vapor phase undergoes rapid hydrolysis in contact with aqueous solvents of high salt concentration and leads to rapid formation of particulate silica. The resulting matrix of silica particles immobilizes the bacterial cells directly on the PHBV/CF surface. For control experiments, PHBV/CF electrodes were incubated with a suspension of DSP-10 as prepared above, but in the absence of TMOS. Cell viability and loading on PHBV/CF electrodes was determined using a microbial cell viability assay based on relative luminescence units (RLU) for direct quantification of ATP according to the manufacturer's instructions (BacTiter-Glo Reagent, Promega, Madison, WI).

Electrochemical Measurements. Electrochemical measurements were made in a one-compartment electrochemical cell containing 30 mL electrolyte (potassium phosphate buffer/KCl, 0.1 M, pH 7.0) with lactate (20 mM) as electron donor (fuel), unless otherwise stated. The experimental cell was assembled from a European 5-neck flask (50 mL) that had three 14/20 slip- fit and two #7 threaded ports for electrodes, gas, and exchange ports (Ace Glass, Vineland, NJ). The electrolyte was purged continuously with nitrogen to displace any dissolved oxygen. Measurements consisted of the PHBV/CF anode as working electrode, a glassy-carbon counter electrode (Metrohm USA, Riverview, FL) and a standard Ag/AgCl reference electrode (CH Instruments Inc., Austin, TX). All electrochemical measurements done with electrolyte at 24−26 °C. Cyclic voltammetry and polarization studies were controlled using a potentiostat (Versastat 3; Princeton Applied Research, Oak Ridge, TN). Power densities were calculated using Ohms law and values normalized to the geometric volume (1.195 cm^3). The internal resistance of the anodes was calculated from the slope of the linear region of the polarization curve (−0.3 to −0.2 V).

Porosity and Contact Angle Measurements. Pore size distribution and surface area was determined using a surface area analyzer (Quantachrome Autosorb-1 analyzer) based on N_2 sorption isotherms. Contact angle measurements were obtained using the sessile drop method with a drop shape analyzer according to the manufacturer's instructions (DSA100 Krűss, Mathews, NC).

Imaging, Sample Preparation, and Microscopy. Scanning electron microscopy (SEM) was used to visualize the interior and exterior features of the composite materials. PHBV/CF anodes with bacteria were fixed with 2.5% glutaraldehyde in cacodylic buffer (0.1M), and then dehydrated in and fixed using ethanol as solvent and critical point drying methods according to the manufacturer's instructions (Autosamdri-815, Tousimis Research Corp. Rockville, MD). Nonconductive samples were sputter-coated with gold (Denton Desk-V, Denton vacuum LLC, Moorestown, NJ). All samples were examined using a model 2600-N scanning electron microscope (Hitachi HTA, Pleasanton, CA).

RESULTS AND DISCUSSION

Fabrication of 3D Hierarchically Structured Polymer/Carbon Bioelectrodes. The composition of the sucrose-based porogen influenced electrode architecture significantly (Figure 1). The crystalline sucrose sieved using 30 mesh (<595 μm) and 45 mesh (<354 μm) were found to optimize material fabrication and structure. Increasing the sucrose mesh size resulted in packed template scaffolds that were too dense for polymer to penetrate. In contrast, decreasing the mesh size of the sucrose (or using sucrose that was not sieved) resulted in a polymer matrix that was poorly interconnected and therefore mechanically brittle. The crystal size of the sucrose defines the porosity within the final structure and dictated the formation of a primarily macroporous/mesoporous internal structure (Figure 1, Table 1). For our trials here as putative MFC applications, an open porous structure is desirable to ensure unrestricted acess of nutrients (fuel) through convective flow and diffusion, combined with large surface area of the porous matrix to encourage interaction between bacterial cells and the anode interface.[9]

Table 1. Materials Characterization of PHBV/CF Composites

	unprocessed carbon nanofibers (CF)	$PHBV_{30}$/CF	$PHBV_{45}$/CF
BET[a] (m^2/g)	ND[d]	4.69	4.41
micropore surface area[b] (m^2/g)	ND	2.906	0.102
conductivity (Ω/g)	20.4	51.2	36.8
EASA[c] (cm^2/g)	ND	697	454
contact angle (deg)	~86.7	~0	~0
density (g/cm^3)	ND	0.14	0.15

[a]BET specific surface area. [b]Micropores <2 nm. [c]EASA: electrochemically accessible surface area. [d]ND: not determined.

In addition, the PHBV/CF composites formed directly around a current collector, thereby providing an electrode that can be fabricated without the need for any further supporting material. The resulting PHBV/CF composite material provides a lightweight structure with a hierarchical porosity as observed in SEM images (Figure 2). The presence of CF within the microstructure of the PHBV composites is evident from SEM images when compared to PHBV polymer prepared in the absence of CF. By initially mixing the CF with the sucrose, the conductive carbon becomes an integral part of the porogen scaffold and creates a homogeneous distribution of carbon throughout the final matrix. The addition of CF also adds a surface roughness to the polymer matrix that increases the surface area (Table 1) and may enhance bacterial adhesison. In addition to SEM, the Barett-Joyner-Halenda method of isotherm analysis was used to characterize the pore size distribution and both PHBV/CF samples were found to have pores in the meso (2−50 nm) and macro (>50 nm) pore range. $PHBV/CF_{45}$ exhibits a well-defined pore size distribution with a maximum distribution at 2−3 nm. $PHBV_{30}$/CF showed less defined pore size distribution over the entire range (2 to 200 nm) with slight domination of 2−3 and 20 nm pores. The Brunauer−Emmett−Teller (BET) method of isotherm analysis was used to determine the specific surface area and confirmed that $PHBV_{30}$/CF and $PHBV_{45}$/CF have overall comparable specific surface areas of 4.69 and 4.41 m^2/g, respectively, despite inherent differences in pore size distribution (Table 1).

The homogeneous distribution of CF throughout the polymer matrix also renders the matrix conductive (Table 1). Bulk and powder resistivity were determined by compressing the materials while measuring the change in resistance and $PHBV_{30}$/CF and $PHBV_{45}$/CF demonstrate a final powder resistivity of 51.2 and 36.8 Ω/g, respectively, compared to an equal mass of pretreated CF (20.4 Ω/g). Using the larger mesh sucrose ($PHBV_{45}$/CF) during fabrication of the composites decreased the amount of nonconductive filler and thereby resulted in a lower resistivity, comparable to plain CF (Table 1). The more defined pore size distribution and the lower

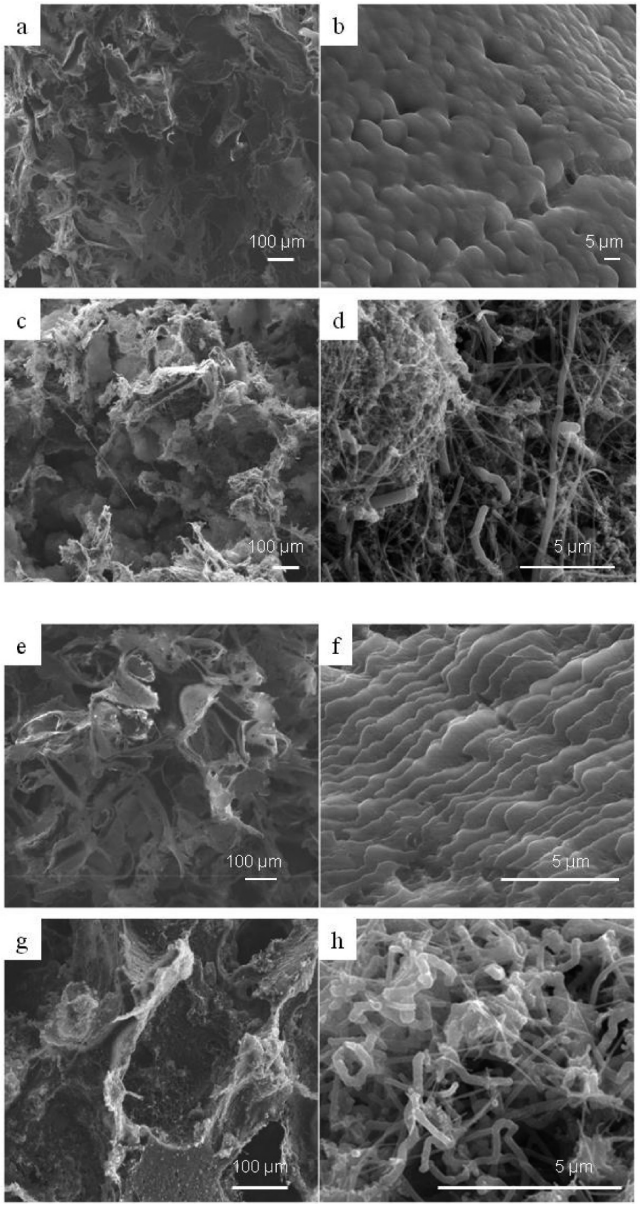

Figure 2. SEM micrographs of cross-sections of PHBV composites with and without CF. (a, b) $PHBV_{30}$, (c, d) $PHBV_{30}$/CF, (e, f) $PHBV_{45}$, (g, h) $PHBV_{45}$/CF.

resistivity made the $PHBV_{45}$/CF the material of choice for this study. While the fabrication of the PHBV/CF composites slightly alters the bulk conductivity of the conductive matrix, the conductivity of the composites is comparable to plain CF. Any reduction in bulk conductivity can be attributed to the meso/macroporosity character of the composite material (Table 1).

Static contact angle measurements of the composites confirmed the hydrophobic nature of the unmodified polymer (contact angle of 106.2 ± 8.7 and 101.1 ± 13.4 for $PHBV_{30}$ and $PHBV_{45}$ mesh respectively, n = 6) in agreement with previous reports.[19] The wetability of the composites increased significantly when CF were included in the structure and decreased the contact angle to essentially zero (Table 1). The additional effective roughness of the CF within the polymer matrix may add to the increased hydrophilicity of the matrix. A similar observation was previously noted when bioactive glass was added to PHB composites.[19]

Characterization of Hierarchically Structured PHBV/CF Electrodes As Anodes for MFC. Initial characterization of the PHBV/CF electrode materials revealed material properties that would be advantageous for MFC applications. To confirm its applicability, we prepared MFC anodes by immobilizing *S. oneidensis* DSP-10 to the surface of PHBV/CF via silica encapsulation.[6] The stabilized open circuit potentials (OCP) of the bacterial anode half-cells were comparable irrespective of sucrose mesh size; −322 ± 18 and −328 ± 16 mV (vs Ag/AgCl) (n = 4) for $PHBV_{30}$/CF and $PHBV_{45}$/CF, respectively (lactate as the electron donor). OCP values were reproducible across replicate electrodes, even when fabricated using different bacterial cultures prepared days or weeks apart. Control anodes in the absence of cells exhibited no electrocatalytic activity besides Faradaic capacitance and OCP of ∼150 mV (vs Ag/AgCl) (data not shown). The high reproducibility of the MFC anodes prepared in this manner is attributed to the porous encapsulation matrix, which serves to create an engineered biofilm of a defined cell density in a specific metabolic state.[6] The short time required to achieve a stable and reproducible MFC anode is advantageous and significantly reduces the time delay (often several days) typically required to establish a natural biofilm and achieve maximum cell potential.[5,9] The physical entrainment of bacterial cells at the anode surface was verified by SEM, which indicated homogeneous distribution when analyzed at various cross sections throughout the matrix (Figure 3). As SEM imaging is only qualitative, quantitative

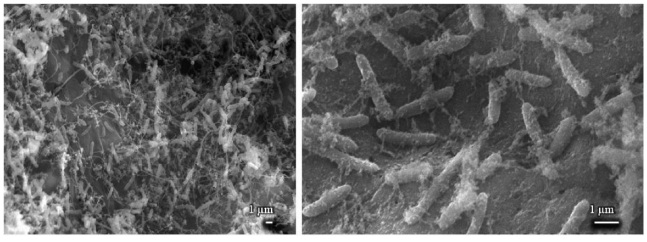

Figure 3. SEM microgaphs of *Shewanella oneidensis* DSP-10 immobilized to PHBV/CF composites via silica vapor deposition.

enumeration of viable microbial cells on the anode was further determined by using ATP as an indicator of metabolically active cells. Cell counts of $2.4 \times 10^7 \pm 1.2 \times 10^7$ and $6.8 \times 10^7 \pm 2.1 \times 10^7$ cfu mg^{-1} polymer were determined for $PHBV_{30}$/CF and $PHBV_{45}$/CF composites, respectively, and confirmed high cell loading on the composite material. Control PHBV/CF electrodes incubated with DSP-10 to allow the formation of a natural biofilm on the electrode surface confirmed that the electrocatalytic characteristics of DSP-10 are reflective of native electron transfer processes and not artifacts of the immobilization procedure (data not shown).

The maximum current density of the DSP-10 functionalized PHBV/CF anodes was comparable irrespective of the template mesh size (22.02 ± 2.37 and 22.18 ± 6.69 $\mu A/cm^3$ [n = 3], for PHB_{30}/CF and $PHBV_{45}$/CF, respectively) and exhibited maximum power densities approaching 5 $\mu W/cm^3$ (4.23 ± 1.22 and 4.38 ± 0.18 $\mu W/cm^3$ [n = 3] for $PHBV_{30}$/CF and $PHBV_{45}$/CF mesh respectively) during polarization measurements (Figure 4). This is in agreement with the hypothesis that the pore-forming/templating ensures the macropore structure and the biological catalyst immobilization capacity is

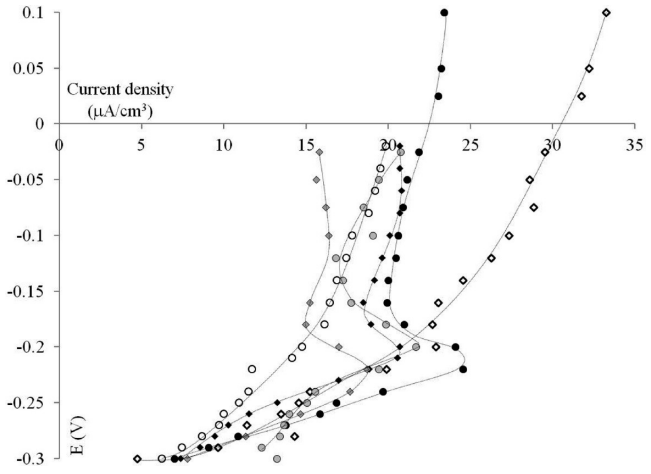

Figure 4. Polarization curves for $PHBV_{30}$/CF (circles), $PHBV_{45}$/CF (diamonds) with immobilized DSP-10.

determined by the meso-porosity obtained from the CF component of the polymer/carbon composite matrix. The internal resistance of the anodes was calculated to be approximately ~10 Ω cm (n = 3) for both $PHBV_{45}$/CF and $PHBV_{30}$/CF.[26] Under potentiostatic conditions (−0.15 V vs Ag/AgCl), $PHBV_{30}$/CF and $PHBV_{45}$/CF anodes maintained a stable current for 8 h with no loss in efficiency, which confirmed the stabilization of the bacterial population at the anode surface (Figure 5). Current density reached a maximum

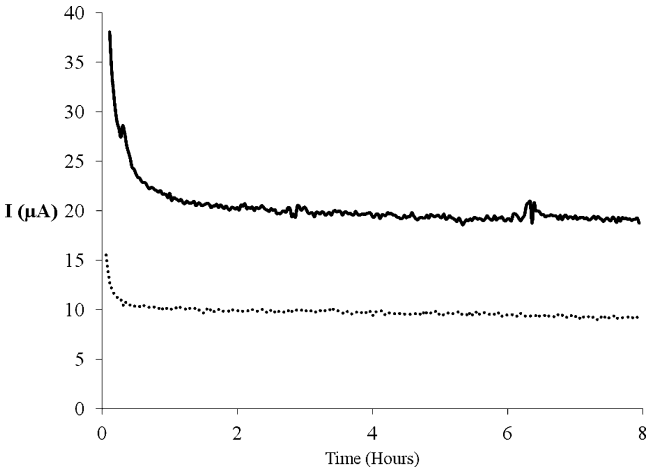

Figure 5. Chronoamperometry of $PHBV_{30}$/CF (dashed line) and $PHBV_{45}$/CF (solid line) at −0.15 V vs Ag/AgCl.

that is sustained between −0.2 and 0 V, and any further increase in current output will likely be limited by mass transport effects. The observed drop in limiting current density after an apparent maximum can be explained by local starvation of the electrodes by a lack of local fuel. This is dictated by the distribution of bacteria within the porous body.

CONCLUSION

Solvent casting methods supported facile fabrication of a conforming, 3D, porous, carbon/polymer material that provided a structure amenable to electrode materials, for example, microbial attachment in an MFC anode. The materials exhibit hierarchical porosity and structure that can be controlled by the size of the porogen and by the characteristics of the conductive component included in the composite. Immobilization of *Shewanella oneidensis* DSP-10 in a CVD grown silica matrix captures the cells in an artificial biofilm that provides rapid and reproducible electrocatalytic activity as evidenced by replicate MFC anodes. The biocompatibility of the PHBV facilitates interaction between the microbial population and the electrode surface and establishes efficient electron transfer between the immobilized biocatalysts and the polymer/carbon electrode interface. The fabrication methodology makes a free form or a cast form anode that can be augmented with various conductive materials to provide interfaces for different redox catalysts (e.g., other microbial strains, redox enzymes for anodic and cathodic reactions), and allow configurations that will conform to system design and various applications. The techniques described herein provided a platform for designing MFC anodes that is versatile and may be extended to alternative biological-based electrode applications.

AUTHOR INFORMATION

Corresponding Author

*Air Force Research Laboratory, AFRL/RXQL, 139 Barnes Drive, Suite # 2, Tyndall Air Force Base, Florida 32403, United States. Phone: (850) 283 6034 (H.R.L.); (850) 283 6223 (G.R.J.). E-mail: heather.luckarift.ctr@tyndall.af.mil (H.R.L.); glenn.johnson@tyndall.af.mil (G.R.J.).

Notes

The authors declare no competing financial interest.

ACKNOWLEDGMENTS

This research was supported at UNM by DOD/AFOSR MURI award (FA9550-06-1-0264) 'Fundamentals and Bioengineering of Enzymatic Fuel Cells'. Research at Tyndall AFB was supporting by funding from the Air Force Office of Scientific Research and the Air Force Research Laboratory, Materials and Manufacturing Directorate.

REFERENCES

(1) Calabrese-Barton., S.; Gallaway, J.; Atanassov, P. *Chem. Rev.* **2004**, *104*, 4867−4886.
(2) Logan, B. E.; Hamelers, B.; Rozendal, R.; Schroder, U.; Keller, J.; Freguia, S.; Aelterman, P.; Verstraete, W.; Rabaey, K. *Environ. Sci. Technol.* **2006**, *40*, 5181−5192.
(3) McLean, J. S.; Majors, P. D.; Reardon, C. L.; Bilskis, C. L.; Reed, S. B.; Romine, M. F.; Fredrickson, J. K. *J. Microbiol. Methods* **2008**, *74*, 47−56.
(4) Yi, H.; Nevin, K. P.; Kim, B.-C.; Franks, A. E.; Klimes, A.; Tender, L. M.; Lovley, D. R. *Biosens. Bioelectron.* **2009**, *24*, 3498−3503.
(5) Biffinger, J. C.; Pietron, J.; Ray, R.; Little, B.; Ringeisen, B. R. *Biosens. Bioelectron.* **2007**, *22*, 1672−1679.
(6) Luckarift, H. R.; Sizemore, S. R.; Roy, J.; Lau, C.; Gupta, G.; Atanassov, P.; Johnson, G. R. *Chem. Commun. (Cambridge, U.K.)* **2010**, *46*, 6048−6050.
(7) Luckarift, H. R.; Nadeau, L. J.; Sizemore, S. R.; Farrington, K. E.; Fulmer, P. A.; Biffinger, J. C.; Johnson, G. R. *Biotechnol. Prog.* **2011**, *27* (6), 1580−1587.
(8) Scott, K.; Rimbu, G. A.; Katuri, K. P.; Prasad, K. K.; Head, I. M. *Trans. IChemE, Part B: Process Safety Environ. Protection* **2007**, *85*, 481−488.
(9) Xie, X.; Hu, L.; Pasta, M.; Wells, G. F.; Kong, D.; Criddle, C. S.; Cui, Y. *Nano Lett.* **2011**, *11*, 291−296.
(10) Lau, C.; Cooney, M. J.; Atanassov, P. *Langmuir* **2008**, *24*, 7004−7010.
(11) Lau, C.; Martin, G.; Minteer, S. D.; Cooney, M. J. *Electroanalysis* **2010**, *22*, 793−798.

(12) Higgins, S.; Cooney, M. J.; Foerster, D.; Minteer, S.; Lau, C.; Atannassov, P.; Cheung, A.; Bretschger, O.; Nealson, K. *Enzym. Microbial Technol.* **2011**, *48*, 458−465.
(13) Logan, B. E.; Cheng, S.; Watson, V.; Estadt, G. *Environ. Sci. Technol.* **2007**, *41*, 3341−3346.
(14) Anderson, A.; Dawes, E. *Microbiol. Rev.* **1990**, *54*, 450−472.
(15) Grage, K.; Jahns, A. C.; Parlane, N.; Palanisamy, R.; Rasiah, I. A.; Atwood, J. A.; Rehm, H. A. *Biomacromolecules* **2009**, *10*, 660−669.
(16) Ahmed, T.; Marcal, H.; Lawless, M.; Wanandy, N. S.; Chiu, A.; Foster, L. J. R. *Biomacromolecules* **2010**, *11*, 2707−2715.
(17) Misra, S. K.; Ansari, T.; Mohn, D.; Valappil, S. P.; Brunner, T. J.; Stark, W. J.; Roy, I.; Knowles, J. C.; Sibbons, P. D.; Jones, E. V.; Boccaccini, A. R.; Salih, V. *J. Res. Soc. Interface* **2010**, *7*, 453−465.
(18) Misra, S. K.; Ansari, T. I.; Valappil, S. P.; Mohn, D.; Philip, S. E.; Stark, W. J.; Roy, I.; Knowles, J. C.; Salih, V.; Boccaccini, A. R. *Biomaterials* **2010**, *31*, 2806−2815.
(19) Misra, S. K.; Mohn, D.; Brunner, T. J.; Stark, W. J.; Philip, S. E.; Roy, I.; Salih, V.; Knowles, J. C.; Boccaccini, A. R. *Biomaterials* **2008**, *29*, 1750−1761.
(20) Misra, S. K.; Nazhat, S. N.; Valappil, S. P.; Moshrefi-Torbati, M.; Wood, R. J.; Roy, I.; Boccaccini, A. R. *Biomacromolecules* **2007**, *8*, 2112−2119.
(21) Misra, S. K.; Ohashi, F.; Valappil, S. P.; Knowles, J. C.; Roy, I.; Silva, S. R.; Salih, V.; Boccaccini, A. R. *Acta Biomater.* **2009**, *6*, 735−742.
(22) Misra, S. K.; Philip, S. E.; Chrzanowski, W.; Nazhat, S. N.; Roy, I.; Knowles, J. C.; Salih, V.; Boccaccini, A. R. *J. Res. Soc Interface* **2009**, *6*, 401−409.
(23) Misra, S. K.; Valappil, S. P.; Roy, I.; Boccaccini, A. R. *Biomacromolecules* **2006**, *7*, 2249−2258.
(24) Sanchez-Garcia, M. D.; Lagaron, J. M.; Hoa, S. V. *Compos. Sci. Technol.* **2010**, *70*, 1095−1105.
(25) Bretschger, O.; Cheung, A. C. M.; Mansfeld, F.; Nealson, K. H. *Electroanalysis* **2010**, *22*, 883−894.
(26) Logan, B. E.; Aelterman, P.; Hamelers, B.; Rozendal, R.; Schroder, U.; Keller, J.; Freguiac, S.; Verstraete, W.; Rabaey, K. *Environ. Sci. Technol.* **2006**, *40*, 5181−5192.